LSD1 Inhibition Prolongs Survival in Mouse Models of MPN by Selectively Targeting the Disease Clone

Jonas S. Jutzi[1,2,3], Maria Kleppe[4,5,6], Jennifer Dias[7], Hans Felix Staehle[1], Kaitlyn Shank[4], Julie Teruya-Feldstein[8], Sudheer Madan Mohan Gambheer[1], Christine Dierks[1], Hugh Y. Rienhoff Jr[7], Ross L. Levine[4,5,6,9], Heike L. Pahl[1,2]

Correspondence: Heike L. Pahl (e-mail: Heike.Pahl@uniklinik-freiburg.de).

Abstract

Despite recent advances, the myeloproliferative neoplasms (MPNs) are attended by considerable morbidity and mortality. Janus kinase (Jak) inhibitors such as ruxolitinib manage symptoms but do not substantially change the natural history of the disease. In this report, we show the effects of IMG-7289, an irreversible inhibitor of the epigenetically active lysine-specific demethylase 1 (LSD1) in mouse models of MPN. Once-daily treatment with IMG-7289 normalized or improved blood cell counts, reduced spleen volumes, restored normal splenic architecture, and reduced bone marrow fibrosis. Most importantly, LSD1 inhibition lowered mutant allele burden and improved survival. IMG-7289 selectively inhibited proliferation and induced apoptosis of $JAK2^{V617F}$ cells by concomitantly increasing expression and methylation of p53, and, independently, the pro-apoptotic factor PUMA and by decreasing the levels of its antiapoptotic antagonist BCL_{XL}. These data provide a molecular understanding of the disease-modifying activity of the LSD1 inhibitor IMG-7289 that is currently undergoing clinical evaluation in patients with high-risk myelofibrosis. Moreover, low doses of IMG-7289 and ruxolitinib synergize in normalizing the MPN phenotype in mice, offering a rationale for investigating combination therapy.

[1]Department of Hematology, Oncology and Stem Cell Transplantation, University Medical Center Freiburg, Center for Tumor Biology, Freiburg, Germany
[2]Spemann Graduate School of Biology and Medicine, University of Freiburg, Freiburg, Germany
[3]Faculty of Biology, University of Freiburg, Freiburg, Germany
[4]Human Oncology and Pathogenesis Program, Memorial Sloan Kettering Cancer Center, New York, NY, USA
[5]Center for Epigenetics Research, Memorial Sloan Kettering Cancer Center, New York, NY, USA
[6]Center for Hematologic Malignancies, Memorial Sloan Kettering Cancer Center, New York, NY, USA
[7]Imago BioSciences, San Francisco, CA, USA
[8]Department of Pathology, Icahn School of Medicine, Mount Sinai, New York, NY, USA
[9]Leukemia Service, Department of Medicine, Memorial Sloan Kettering Cancer Center, New York, NY, USA.

Introduction

Philadelphia-negative myeloproliferative neoplasms (MPNs) comprise a group of clonal malignant hematological diseases that includes essential thrombocythemia (ET), polycythemia vera (PV), and primary myelofibrosis. At various rates, ET and PV patients can develop myelofibrosis (MF) and all 3 MPNs can transform to acute myelogenous leukemia (AML), events associated with considerable morbidity and mortality. To date, bone marrow (BM) transplantation remains the only potentially curative therapy for MPN patients.

The discovery of mutations in *JAK2*, *MPL*, and *CALR*, all of which activate the STAT signaling pathways, led to the development of the first targeted therapy for MPN, the JAK1/2 inhibitor ruxolitinib, approved for the treatment of MF and hydroxyurea-resistant PV. Ruxolitinib improves constitutional symptoms and reduces spleen volumes. As ruxolitinib proved equally effective in patients with wt JAK2, it has been proposed that it exerts its effect in part by lowering inflammatory cytokine levels.[1,2] Importantly, ruxolitinib only modestly reduces the mutant *JAK2* allele burden in a minority of patients. Likewise, disease progression is slowed only in some patients.[3–7] Recently, Newberry et al reported that 22/63 (36%) of MF patients acquired new mutations while on ruxolitinib therapy, 15/22 (68%) of these in ASXL1, which have been associated with an inferior survival.[8,9] The modest effects on clinical outcomes and potential selection of a more aggressive clone underscore the need for more effective therapies, especially those that impact the underlying malignancy by selectively reducing the malignant population.

LSD1 modifies chromatin by removing mono- and dimethyl groups from histone H3 with the effect of epigenetically regulating gene transcription. Enzyme activity is essential for

steady-state hematopoiesis as genetic knockdown or pharmacologic inhibition of LSD1 inhibits thrombopoiesis, erythropoiesis, and granulopoiesis.[10,11] The hematologic effects of LSD1 inhibition (LSD1i) are fully reversible and chronic treatment is not associated with impairment of long-term BM function (Sprussel et al[10] and Imago BioSciences, unpublished).

The hematopoietic effects of LSD1i suggest that this may constitute a therapeutic option in MPN. Several clinical findings support this hypothesis. First, LSD1 is overexpressed in patients with MPN and AML.[12] Second, LSD1 is necessary for sustaining the self-renewal potential of leukemic stem cells as its depletion by RNAi attenuated MLL-AF9-driven leukemia.[13,14] Finally, LSD1i led to stem cell reprogramming resulting in myeloid differentiation and a reduction of AML cell engraftment, an effect enhanced by the addition of all-*trans* retinoic acid.[14] Together these observations suggest that LSD1i might be successful in safely controlling the proliferative features of MPNs and potentially reducing the mutant clone burden.

In this report, we investigate the consequences of LSD1i in mouse models of MPN. We provide evidence that many cardinal MPN features—erythrocytosis, leukocytosis, thrombocythemia, hepatosplenomegaly, and elevated inflammatory cytokines—can be significantly improved by oral treatment with the LSD1 inhibitor IMG-7289. We show that the mutant allele frequency is reduced and overall survival improved with this treatment regimen. Moreover, LSD1i synergized with JAK1/2 inhibition in ameliorating the MPN phenotype. Finally, we describe the mechanism by which LSD1i achieves these effects. IMG-7289 is currently undergoing clinical evaluation in both AML and MF (NCT02842827 and NCT03136185).

Results

Mice carrying the *Jak2*[V617F] mutation as an inducible, floxed allele 3' to the endogenous *Jak2* locus (L2-strain[15]) were crossed with mice expressing the Cre recombinase under control of the interferon-inducible *Mx1* promoter to generate a novel *Jak2*[V617F] mouse model. Expression of Cre recombinase in F$_1$*Mx1cre-Jak2*[V617F] mice (*Mx-Jak2*[V617F]) leads to excision of the wild type (WT) *Jak2* allele and expression of the mutant *Jak2*[V617F] allele encoding the constitutively activated Jak2. Due to the leakiness of the *Mx1* promoter,[16]*Mx1cre-Jak2*[V617F] mice develop an MPN phenotype without induction of *Mx1* by poly(I:C) injections.

We chose the Mx1 promoter as it responds to proinflammatory stimuli. Evidence is mounting that chronic inflammation contributes both to the initiation and to the maintenance of MPN.[17,18] A substantial proportion of the therapeutic effect of ruxolitinib is thought to derive from the reduction in inflammatory cytokine levels, hence its effect on patients expressing wt JAK2.[1,19] In our model, the expression of Jak2[V617F], by inducing inflammation, will perpetuate and exacerbate disease status, similar to the current model implicating inflammation in promoting disease progression in MPN patients.

By the age of 6 weeks, *Mx-Jak2*[V617F] mice display mild erythrocytosis with reticulocytosis, thrombocytosis and mild leukocytosis (Fig. 1, data at day 0). The MPN progresses over time in untreated animals: by day 56, the mean white blood cell (WBC) counts exceeded 50,000 cells/μL, neutrophilia increased 4-fold, platelet counts rose above 3000×10^6/μL, and the hematocrit reached 70%, despite a relatively low *Jak2*[V617F] allele burden, determined by qPCR of peripheral blood (3–15%, Fig. S1A, Supplemental Digital Content, http://links.lww.com/HS/

A13). Concomitant presence of WT and mutant cells, characteristic of virtually all MPN patients, allows the assessment of a possible selective effect of LSD1i.

Cohorts consisting of 8 mice equal in age, sex, and blood counts were dosed once daily with either IMG-7289 (45 mg/kg body weight) or vehicle for 56 days. Complete blood counts (CBC) were assessed at 14-day intervals. Treatment with IMG-7289 normalized neutrophil count within 14 days and the WBC count, hematocrit, reticulocytosis, and monocytosis were also significantly reduced over the course of treatment compared to controls (Fig. 1) albeit remaining slightly above normal. LSD1 activity is required for full megakaryocyte maturation and platelet production[10,11] and the effect of LSD1i on platelet production is dose dependent (Imago, unpublished). At the chosen dose of 45 mg/kg per d of IMG-7289, platelet counts were dramatically decreased (Fig. 1B). Nonetheless, treated mice did not exhibit spontaneous bleeding nor was there any evidence of hemorrhage at autopsy (data not shown).

Splenomegaly secondary to extramedullary hematopoiesis (EMH) is a prominent feature of MPN that contributes to poor quality of life. In this *Mx-Jak2*[V617F] model of MPN, mice developed severe splenomegaly (up to 10-fold increase in spleen weight). Splenic architecture was completely destroyed, eliminating demarcation of the white and red pulp (Fig. 2A, left). IMG-7289 treatment significantly reduced splenomegaly (Fig. 2B) with a few treated mice normalizing their spleen weight. Remarkably, the 56-day course led to partial restoration of lymph follicles and spleen architecture by histological examination (Fig. 2A, right).

Another frequent finding in MPN patients is BM fibrosis presenting either as primary MF or developing secondarily during MPN disease progression. The *Mx-Jak2*[V617F] mouse model, however, does not develop appreciable fibrosis before mice become moribund. We therefore employed a second well-characterized mouse model of MPN in which the mutant thrombopoietin receptor, *MPL*[W515L], is transduced into hematopoietic stem/progenitor cells.[20] In contrast to the PV-like disease observed in the *Jak2*[V617F] mouse model, *MPL*[W515L]-diseased mice develop an ET/MF-like disease with fulminant BM fibrosis. Treatment of *MPL*[W515L] mice with the LSD1 inhibitor IMG-98, a molecule with an identical pharmacophore to IMG-7289, led to marked reduction in BM reticulin fibrosis after 4 weeks of treatment (Fig. 2C). Similar to the response in *Mx-Jak2*[V617F] animals, LSD1i partially restored splenic architecture and diminished EMH in the liver (Fig. S1B-I, Supplemental Digital Content, http://links.lww.com/HS/A13). These data in 2 distinct models of MPN show that LSD1i results in significant improvement in the most important clinical signs and symptoms of MPNs.

The only Food and Drug Administration approved therapy for MPN is the JAK1/2 inhibitor ruxolitinib. While this agent can bring elevated hematologic parameters into the normal range and reduce splenomegaly in MPN patients, it has limited disease-modifying activity including only modest reduction of the *JAK2*[V617F] allele burden.[3–7] Ruxolitinib is not selective for the mutant kinase and thus does not selectively target *JAK2*[V617F]-expressing cells. Given that LSD1 selectively inhibits the self-renewal of leukemia initiating cells,[13] we asked whether IMG-7289 had a differential effect on mutant versus WT cells. As our mouse model contains both WT and *Mx-Jak2*[V617F] cells, we used qPCR to determine the *Jak2*[V617F] allele burden at day 14 and after 56 days of IMG-7289 treatment. Figure 2D shows that in vehicle-treated mice, the *Jak2*[V617F] allele burden increases over 56 days consistent with published reports that the *Jak2*[V617F]
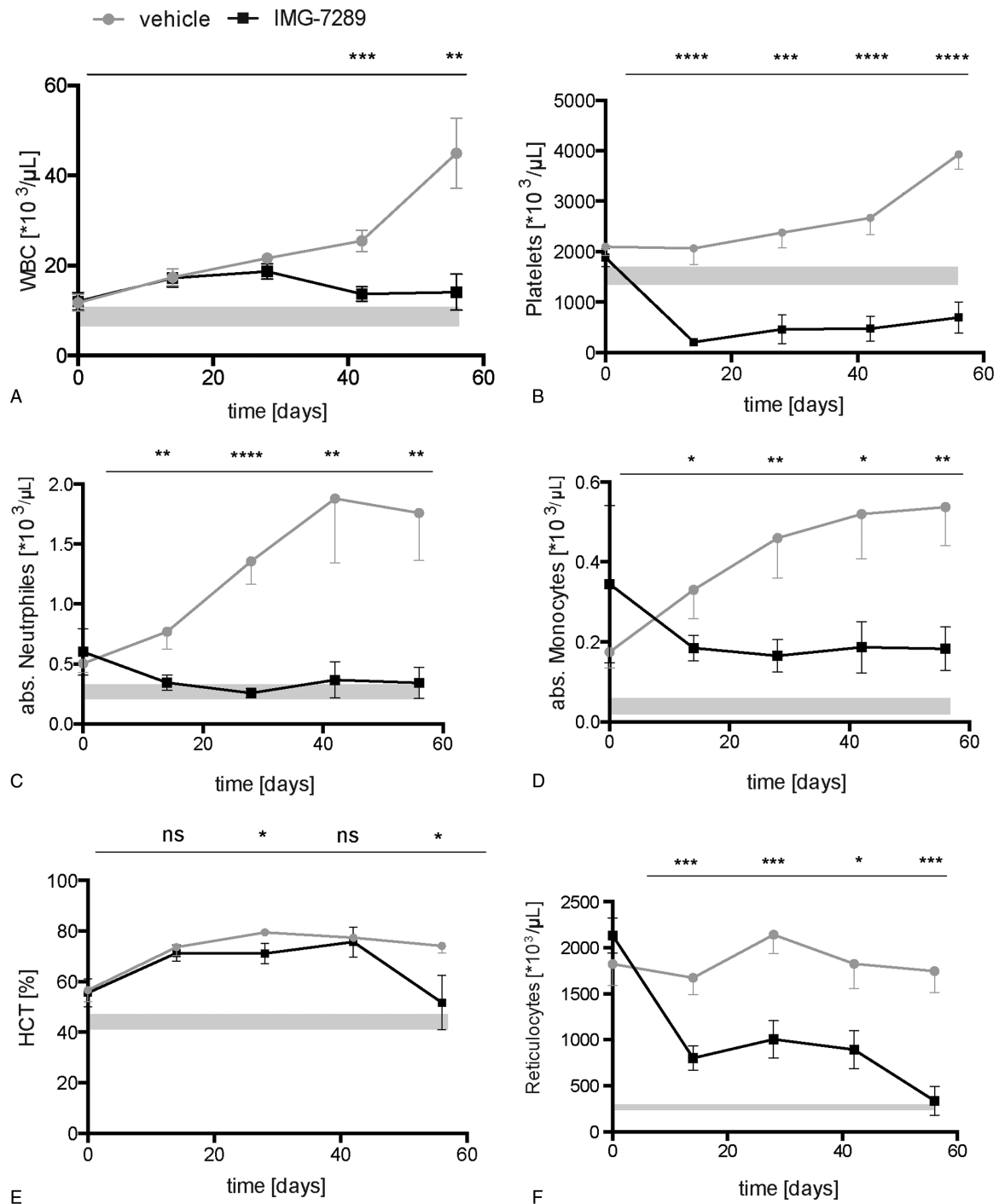
Figure 1. Hematological parameters of Jak2^V617F mice treated with the LSD1 inhibitor IMG-7289. Peripheral blood was obtained by retrobulbar puncture and analyzed on an Advia 120 system at the indicated time points (n = 8 mice per group). Mean and standard error of mean are shown. (A) White blood cell (WBC) count, (B) platelet counts, (C) absolute neutrophil count (ANC), (D) absolute monocyte count, (E) hematocrit (HCT), and (F) absolute reticulocyte count. Statistical analysis was conducted using Student t tests. $^*P < 0.05$, $^{**}P < 0.01$, $^{***}P < 0.001$, $^{****}P < 0.0001$ versus vehicle-treated mice.

mutation confers a selective growth advantage to hematopoietic stem/progenitor cells causing expansion of the mutant cell population.[15] Conversely, LSD1i significantly decreased the Jak2^V617F allele burden in both peripheral blood and spleen cells (Fig. 2D), strongly suggesting that Jak2^V617F cells are more sensitive to LSD1i than their WT counterparts.

Our mouse model is driven by Mx1-Cre mediated expression of the Jak^V617F allele. Since the Mx1 promoter is induced by

inflammatory stimuli, we were concerned that LSD1i mediated suppression of inflammation rather than specific inhibition of Jak2^V617F expressing cells was responsible for the observed reduction in allele burden. To investigate this possibility, we employed a different Jak2^V617F model, mice transplanted with BM retrovirally transduced to express both GFP and Jak2^V617F.[21,22] Mice with established disease were treated for 14 consecutive days with 45 mg/kg IMG-7289. The proportion of
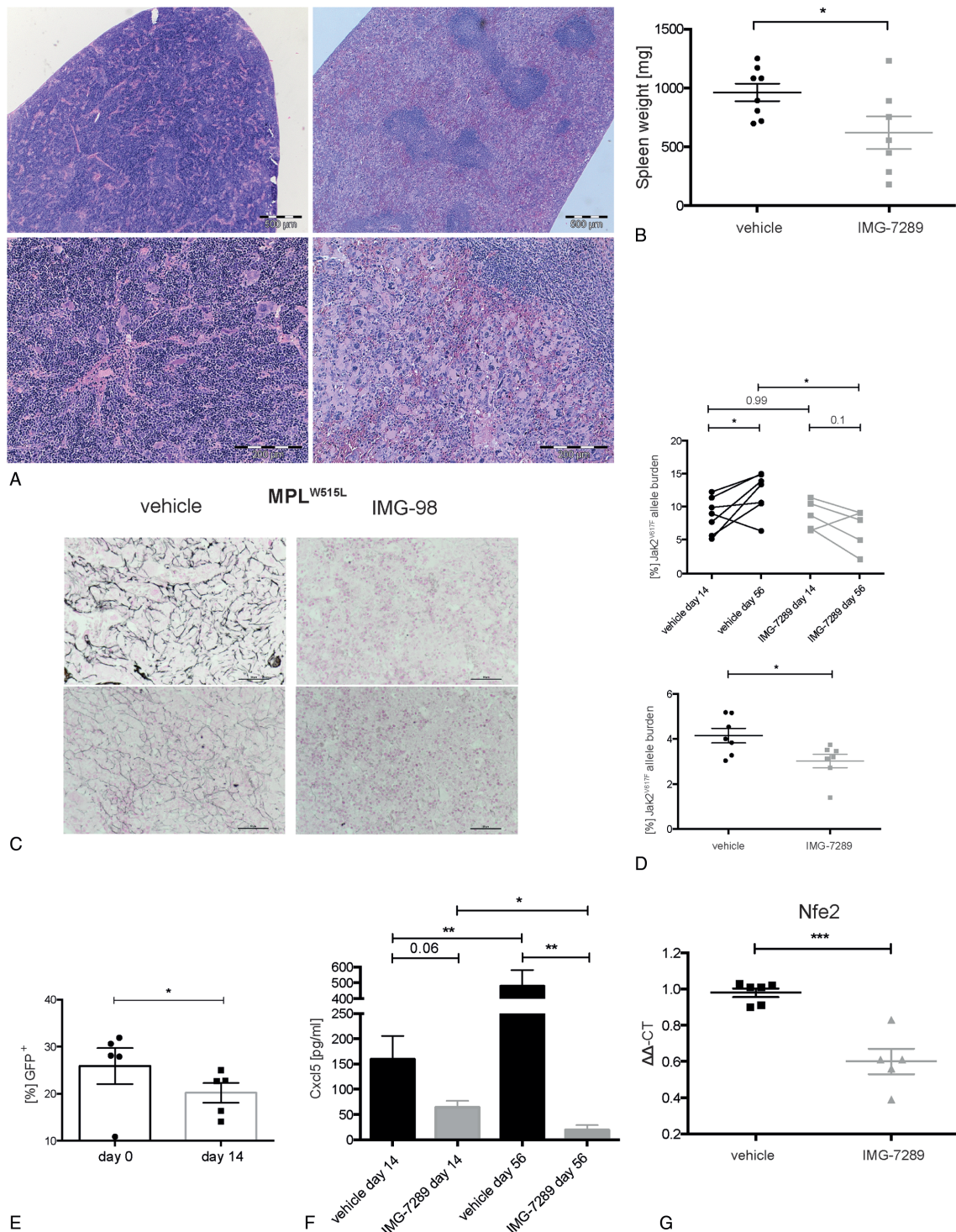
Figure 2. Effect of LSD1 inhibition on inflammation, spleen size, allele burden, and fibrosis. (A) Representative presentation of vehicle (left) and IMG-7289-treated (right) spleen. Top bars: 500 μm; bottom: higher magnification of the same spleens, bars: 200 μm H&E staining of formalin-fixed and paraffin-embedded spleen. (B) Spleen weight of vehicle or IMG-7289 treated Jak2^{V617F} mice. n=7 to 8 per group, as indicated. (C) Representative presentation of 2 vehicle (left) and 2 IMG-98-treated (right) bone marrows. Staining for reticulin fibers using silver impregnation. Bars: 50 μm. (D) *Jak2*^{V617F} mutant allelic burden in vehicle- and IMG-7289-treated peripheral blood cells, obtained at days 14 and 56 of treatment, respectively (top), as well as treated splenic cells (bottom). Mean and standard error of mean are shown. (E) Percentage of GFP positive (*Jak2*^{V617F}) donor peripheral blood cells of bone marrow transplanted mice. (F) Cxcl5 levels in plasma samples obtained at days 14 and 56 of treatment measured by ELISA. (G) RNA was isolated from BM of vehicle- and IMG-7289-treated mice and subjected to quantitative RT-PCR analysis for *Nfe2* and *ß2-microglobulin* as a control. Relative RNA expression was determined by −ΔΔCT and expression of vehicle-treated BM was set to 1.0. (D–F) n=4 to 8, as indicated. Statistical analysis was conducted using Student *t* tests. *P < 0.05, **P < 0.01, ***P < 0.001. BM=bone marrow.

GFP-positive donor cells in the peripheral blood decreased significantly over this short period of time (Fig. 2E), demonstrating the LSD1i reduced the burden of the neoplastic clone. These data offer the possibility of a therapeutic window in which the remaining, normal hematopoietic cells are spared during LSD1i therapy in MPN patients.

Serum levels of several inflammatory cytokines are increased in MPN patients including interleukin 8 (IL8), the most consistently elevated cytokine in MF.[23] In MF patients, IL8 levels constitute an independent prognostic indicator, correlating inversely with leukemia-free survival. The effect of IMG-7289 on serum levels of Cxcl5, a murine ortholog of IL8 made in megakaryocytes, was determined. LSD1i reduced Cxcl5 levels by 60% after 14 days of treatment and by more than 95% after 56 days of treatment compared to vehicle-treated mice (Fig. 2F). LSD1i had a similar effect of reducing serum Cxcl5 in the MPL^{W515L} mouse model (Fig. S1L, Supplemental Digital Content, http://links.lww.com/HS/A13).

The mechanism by which LSD1 depletion causes a decrease in platelet production is only incompletely understood but the recruitment of LSD1 to chromatin by the transcription factor GFI1b is essential for megakaryocyte development and function.[24] Another transcription factor, Nfe2, is also essential for thrombopoiesis in mice; *Nfe2* null mice show severe thrombocytopenia at birth and die perinatally from hemorrhage.[25] Conversely, overexpression of *Nfe2* in results in thrombocythemia.[26,27] Nfe2 is also required for other megakaryocytic functions including the production of IL8.[28] NFE2 is overexpressed in a majority of MPN patients.[29,30] We therefore determined the effects of LSD1i on *Nfe2* mRNA expression in BM cells of IMG-7289-treated mice. *Nfe2* levels were significantly reduced compared to untreated animals (Figs. 2G and S1K, Supplemental Digital Content, http://links.lww.com/HS/A13). This effect was not due to a reduction in the number of megakaryocytes or megakaryocyte progenitors (MEPs) (Figs. 2A and 3H). These data link the effects of LSD1i to altered expression of a transcription factor critical to megakaryocytic function including thrombopoiesis and cytokine production.

FACS analysis of stem and progenitor compartments in the BM revealed an increase in the Lin$^-$/Sca$^+$/Kit$^+$ (LSK) compartment following IMG-7289 treatment (Fig. 3A). This was due to an expansion of the CD135$^-$ CD90.1$^-$ CD34^{lo} LSK-subpopulation
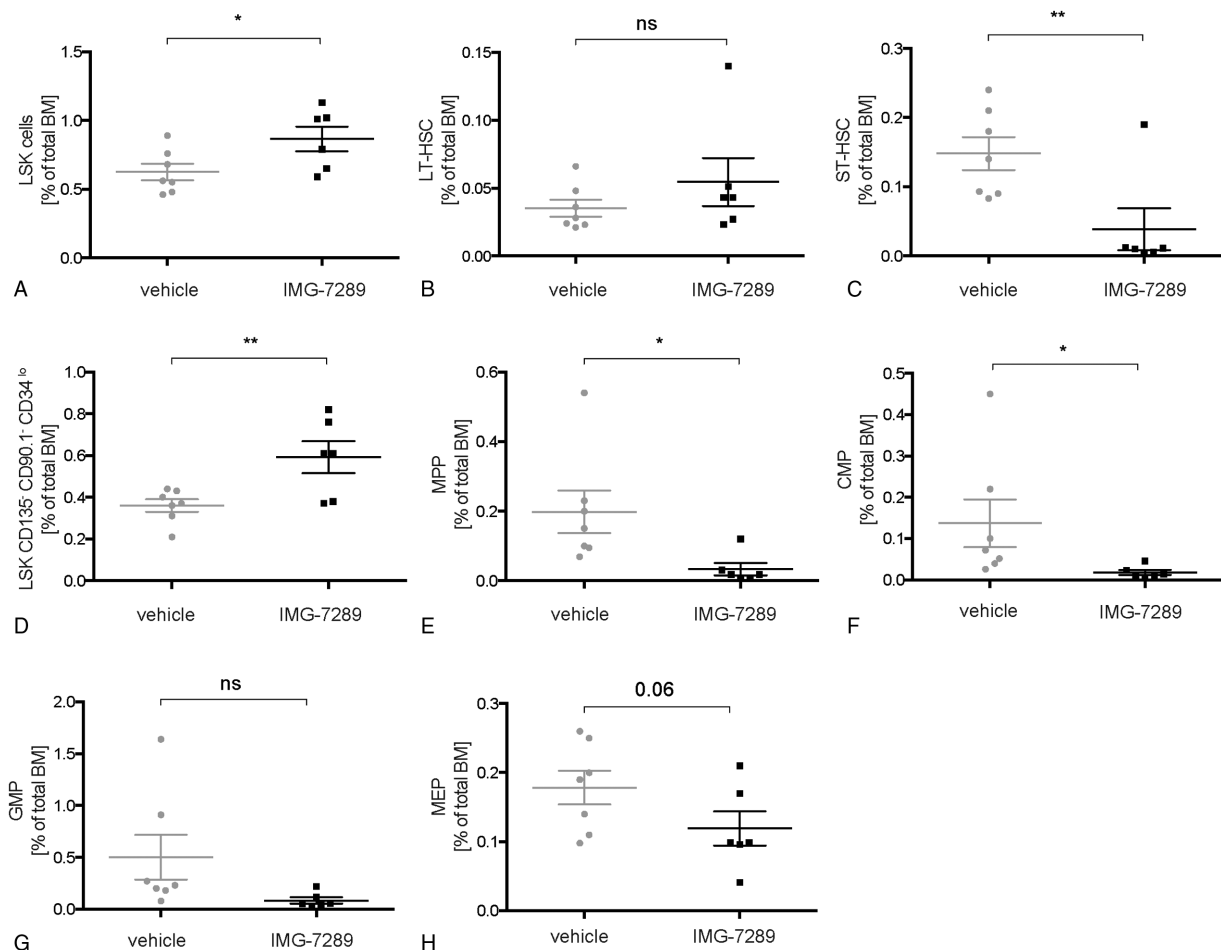

Figure 3. Effect of LSD1 inhibition on lineage commitment and hematopoietic stem and progenitor populations in $Jak2^{V617F}$ mice. (A–H) BM cells were stained with antibodies against a cocktail of lineage markers as well as against c-kit, Sca-1, CD34, Fc-γR, and Flt3/Flk2. All given subpopulations, defined as previously described,[51,52,55] are depicted as a percentage of total BM cells. (A) Lineage$^-$, c-kit$^+$, Sca-1$^+$ (LSK) cells. (B) Long-term hematopoietic stem cell (LT-HSC: LSK, CD34^{neg}, FLK2/FLT3^{neg}). (C) Short-term hematopoietic stem cell (ST-HSC: LSK, CD34^{int}, FLK2/FLT3^{neg}). (D) Lineage$^-$, c-kit$^+$, Sca-1$^+$, CD135$^-$, CD90.1$^-$, CD34^{lo} cells. (E) Multipotent progenitor (MPP). (F) Common myeloid progenitor (CMP). (G) Granulocyte-macrophage progenitor (GMP). (H) Megakaryocyte-erythrocyte progenitor (MEP). (A–H) n=6 to 7 per group, as indicated. Mean and standard error of mean are shown. Statistical analysis was conducted using Student *t* tests. $^*P < 0.05$, $^{**}P < 0.01$ versus vehicle-treated mice. BM = bone marrow.

(Fig. 3D). Interestingly, all other stem and progenitor cell compartments were either not significantly increased (long-term hematopoietic stem cell [LT-HSC], Fig. 3B) or decreased (short-term HSCs [ST-HSCs], multipotent progenitors [MPPs], common myeloid progenitors, granulocyte-macrophage progenitors, and MEPs [Fig. 3C, E–I]). These data are in contrast to the observation that shRNA-mediated partial depletion of LSD1 in healthy mice caused a dramatic increase in several stem and progenitor compartments.[10] Pharmacological inhibition of LSD1 did not cause a significant expansion of immature cells in the BM of MPN mice.

The data presented in Figure 1 show that IMG-7289 treatment ameliorates and normalizes CBCs in young mice displaying the full MPN phenotype. This therapeutic strategy approximates treating MPN patients at diagnosis or early during their disease course. However, many patients, especially ET and PV patients, can initially be managed with little or no medical intervention. In order to model the treatment of MPN patients with longer disease duration, we asked whether overall survival in mice with more advanced disease could be improved with LSD1i. Mx-$Jak2^{V617F}$ animals at 13 weeks of age display advanced disease and survive only for a median of 2 to 5 weeks. Treatment beginning at week 13 with IMG-7289 showed a striking improvement in survival. While none of the vehicle-treated mice survived the duration of the study, dying of spontaneous thoracic or abdominal hemorrhage, no mouse receiving daily IMG-7289 succumbed to this ET/PV phenotype during the 75-day treatment period ($P <$ 0.01, Fig. 4A).

Reduction of the $Jak2^{V617F}$ allele burden and the accompanying increase in survival can be explained either by a decrease in proliferation of $Jak2^{V617F}$ cells, or by an increase in apoptosis, or both. We therefore determined the effect of IMG-7289 on apoptosis in SET-2 cells, a cell line derived from a $Jak2^{V617F/+}$ patient with post-ET-AML.[31] LSD1i caused a dose-dependent increase in apoptosis as indicated by Annexin V/PI staining (Fig. 4B–D). This was accompanied by a highly significant decrease in expression of the antiapoptotic protein BCL$_{XL}$ (Fig. 4E and F). BCL$_{XL}$ has previously been shown to be overexpressed in primary erythroid cells from patients with PV.[32] Increased BCL$_{XL}$ expression may contribute to EPO-independent growth manifested by the formation of "EPO-independent colonies, EECs," which are pathognomonic for this disease.[32] Normalization of BCL$_{XL}$ levels by LSD1i may thus constitute 1 mechanism by which this therapy selectively targets the malignant clone.

LSD1 has been demonstrated to demethylate proteins other than histones, thereby modulating their activity.[33] Activity of the TP53 protein is repressed by LSD1-mediated demethylation of lysine 370. Methylated TP53 (TP53 K370me2) is significantly more active in inducing apoptosis than unmethylated TP53.[34] We therefore investigated whether IMG-7289 treatment affects TP53K370 methylation as well as total TP53 expression. LSD1i caused both a significant increase in the amount of dimethylated TP53 and in the total TP53 protein level (Fig. 4G and H).

TP53 regulates both the expression of BCL$_{XL}$ as well as of its pro-apoptotic antagonist p53 upregulated modulator of apoptosis (PUMA).[35–37] However, the SET-2 cells used carry a homozygous p53 mutation, R248W.[38] While this mutation confers a neomorphic function[39] rather than a mere loss of function, its potential to activate p53 target genes may be lost. Nonetheless, in SET-2 cells, IMG-7289 treatment decreased levels of the antiapoptotic protein BCL$_{XL}$ and increased levels of the pro-apoptotic protein PUMA (Fig. 4E and I). Both BCL$_{XL}$ and

PUMA can also be regulated by p53-independent pathways.[40,41] IMG-7289 thus exerts a pro-apoptotic effect on 3 key regulators of programmed cell death, TP53, BCL$_{XL}$, and PUMA. The decrease in $Jak2^{V617F}$ allele burden observed in our mouse model suggests that this effect of LSDi is more pronounced in cells carrying the active $Jak2^{V617F}$ allele.

We addressed the possible selectivity for $Jak2^{V617F}$ positive cells in an additional model system. We cocultured murine Baf/3 cells expressing the endogenous WT $Jak2$ with Baf/3 cells expressing $Jak2^{V617F}$ through retroviral transduction. In this system, WT and $Jak2^{V617F}$ expressing cells can thus be distinguished by GFP positivity. We determined the rate of apoptosis of wt and $Jak2^{V617F}$ cells by Annexin V/PI staining. IMG-7289 treatment caused a statistically highly significant and dose-dependent increase in apoptosis of $Jak2^{V617F}$ Baf/3 cells over Baf/3 WT cells (Fig. 4K). This finding suggests that cells with constitutively active Jak2 signaling are more prone to undergo apoptosis following LSD1i, than WT cells, which are affected only marginally.

To test, whether a reduction of $Jak2^{V617F}$ allele burden is caused both by the induction of apoptosis as well as a concomitant decrease in proliferation, we performed cell cycle analysis. SET-2 cells treated with IMG-7289 show a statistically significant reduction of cells in S-phase compared with control (Fig. 4L). The proportion of cells in G2M and G0/1 phase was increased but this change did not reach statistical significance. Hence, LSD1i blocks G1/S transition thereby arresting cell cycle progression. These data suggest that both IMG-7289-induced apoptosis in $Jak2^{V617F}$ cells and the delay in cell cycle progression play a role in reducing the $Jak2^{V617F}$ allele burden.

As LSD1 demethylates mono- and dimethylated histone 3 at lysine 4[42] and at lysine 9,[43] we investigated the effect of IMG-7289 treatment on global H3K4me3 and H3K9me2 levels in BM of Mx-$Jak2^{V617F}$ mice. Treatment with IMG-7289 significantly increased global levels of both H3K4me3 and H3K9me2 indicating that LSD1 plays a major role in modulating the methylation status of these 2 histone sites in BM cells (Fig. 5A and B). Moreover, these data show that other histone demethylases do not appear to compensate for LSD1i. The lack of compensatory epigenetic mechanisms suggests that tachyphylaxis or resistance to LSD1i is unlikely, making LSD1 an especially attractive pharmacological target.

To date, ruxolitinib is the only targeted therapy approved for MPN patients. However, Newberry et al recently reported that 22/62 (36%) of MF patients acquired new mutations while on ruxolitinib therapy.[8] The most frequently acquired mutation was in ASXL1 (15/22=68%), which is concerning, as ASXL1 mutations are associated with inferior survival in MPN.[9] Limiting the exposure to ruxolitinib may lower the selective pressure, reducing the rate at which new mutations emerge. Maximal dose reduction could be achieved if ruxolitinib could be combined with a synergistically acting second agent, as synergy potentiates the effects of low drug concentrations.

We therefore investigated potential synergism between Jak1/2 and LSD1i by determining the effect of low doses of ruxolitinib, IMG-7289, or the combination of both drugs on colony formation of SET-2 cells in methylcellulose. While 25 nm IMG-7289 alone significantly reduced colony formation, 175 nm ruxolitinib had almost no effect (Fig. 6A). The combination of both drugs decreased SET-2 cell colony formation to a far greater extent than IMG alone or than the amount expected from an additive effect (Fig. 6A), suggesting that ruxolitinib and IMG-7289 indeed synergize in inhibiting $JAK2^{V617F}$-driven prolifera-
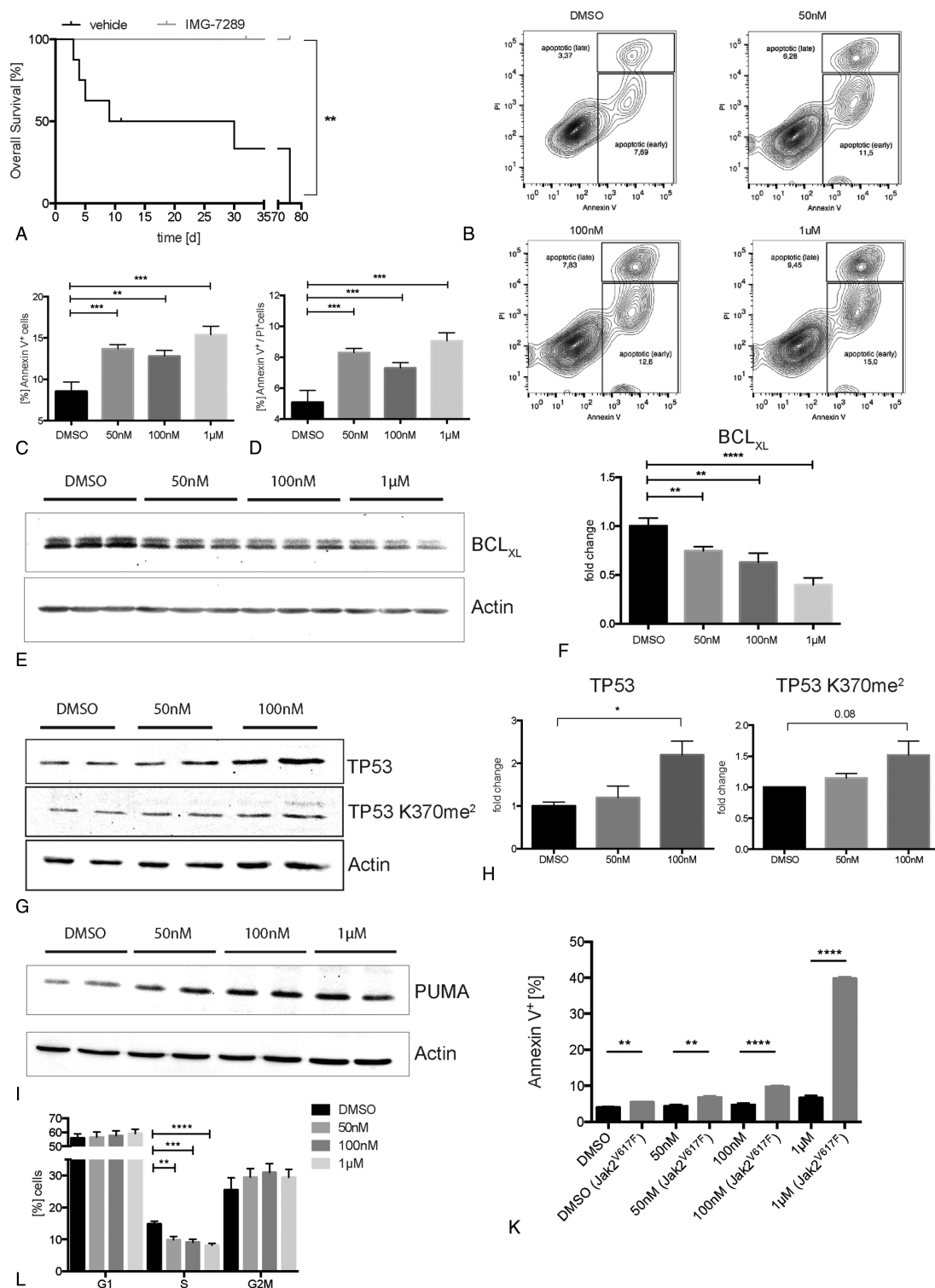
Figure 4. LSD1 inhibition with IMG-7289 enhances survival, induces apoptosis via BCL$_{XL}$ and PUMA in a TP53-dependent manner, and leads to cell cycle arrest. (A) Overall survival of Jak2^{V617F} mice treated with IMG-7289 in an advanced stage of disease. Statistical analysis was conducted using Log-rank (Mantel-Cox) test. (B–F) SET-2 cells, treated either with DMSO or 50 nM, 100 nM, and 1 μM IMG-7289, respectively. n = 3 independent experiments, each performed in triplicate. (B) Representative FACS plots of SET-2 cells stained for Annexin V/PI, after 96 hours of treatment. (C + D) Quantification of apoptosis shown in (B) detected by either Annexin V (C) or Annexin V and PI staining (D). (E) Representative western blot showing BCL$_{XL}$ protein levels (top) and actin as loading control (bottom) of treated SET-2 cells. (F) Quantification of BCL$_{XL}$ protein levels shown in (E). (G) Representative western blot showing protein levels of TP53 (top) and TP53 K370me^2 (middle) and actin as loading control (bottom) in treated SET-2 cells. (H) Quantification of TP53 and TP53 K370me^2 (middle) protein levels, shown in (G). (I) Representative western blot showing PUMA protein levels (top) and actin as loading control (bottom) of treated HEK293 cells. (K) Quantification of apoptosis in cocultures of Baf/3 wild type and Baf/3 Jak2^{V617F} cells, treated with IMG-7289 or a DMSO control, detected with FACS by Annexin V staining. n = 2 independent experiments (each in duplicate). (L) Hoechst-based cell cycle analysis of treated SET-2 cells. n = 2 independent experiments (each in triplicate). (C, D, F, H, I, K) Mean and standard error of mean are shown. Statistical analysis was conducted using Student t tests. $^*P < 0.05$, $^{**}P < 0.01$, $^{***}P < 0.001$, and $^{****}P < 0.0001$.
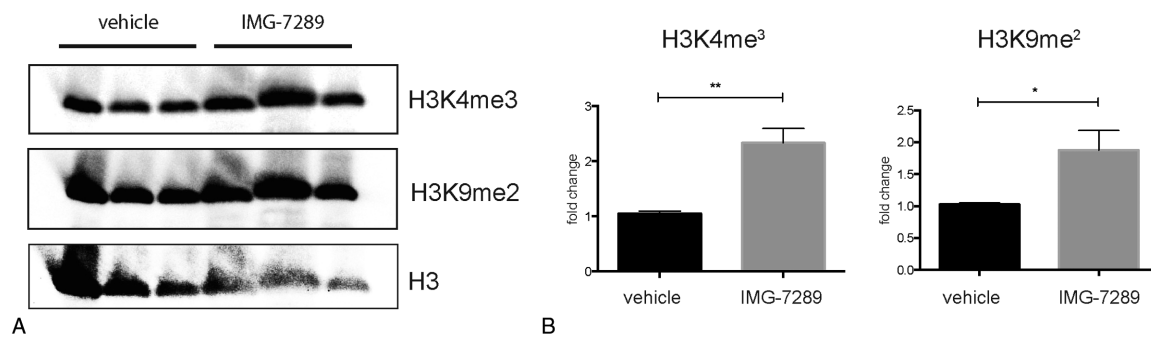
Figure 5. LSD1 inhibition increases global histone 3 K4 and histone 3 K9 methylation levels in bone marrow cells. (A) Western blot showing protein levels of histone 3 lysine 4 trimethylation (top), histone 3 lysine 9 dimethylation (middle), and total histone 3 (bottom, loading control). (B) Quantification of histone 3 lysine 4 trimethylated and (left) and histone 3 lysine 9 dimethylated protein. n = 3 in triplicate. Statistical analysis was conducted using Student *t* tests with Welch correction. *$P < 0.05$ and **$P < 0.01$.

tion. Decrease SET-2 cell proliferation was due to a significant increase in the percentage of apoptotic cells when suboptimal concentrations of the drugs were combined (Fig. 6B).

Next, we determined whether IMG and ruxolitinib also synergize in vivo. Cohorts consisting of 7 to 8 *MxJak2^{V617F}* mice, equal in age, sex, and blood counts were treated with vehicle, IMG-7289 (15 mg/kg body weight, once daily) or ruxolitinib (30 mg/kg body weight, b.i.d.) alone or in combination for 42 days. CBCs were assessed at 14-day intervals. While treatment with either ruxolitinib or IMG-7289 alone stabilized or slightly decreased the leukocyte count, the combination of both drugs normalized leukocyte counts within 14 days of treatment, clearly demonstrating synergism of this low-dose combination regimen (Fig. 6C, left, the gray bar indicates the range of normal blood values of WT littermate controls).

Platelet counts were reduced mildly by ruxolitinib alone but normalized either by IMG-7289 alone or by the combination treatment (Fig. 6C, second from the left). While the thromboreductive effect is thus not synergistic, it is important to note that thrombocytopenia was neither pronounced nor exacerbated by the low-dose drug combination. By contrast, at doses of 45 mg/kg of IMG-7289, platelet counts were dramatically decreased (Fig. 1B), strengthening the finding, that the effect of LSD1i on platelet production is dose dependent rather than due to unspecific toxicity.

The effect of all 3 treatment regimen on red blood cell (RBC) number was mild, but, by the end of treatment, statistically significantly larger with the drug combination than with the single agents (Fig. 6C, second to right). More importantly, the reticulocyte count, a measure for the erythropoietic activity, normalized in both IMG-7289 and combination treated mice at day 42 (Fig. 6C, right). Given the extended life span of erythrocytes (63 days in mice) normalization of the reticulocyte count is predicted to lead to normal RBC numbers with longer follow-up.

As the abnormal CBCs in MPN patients and murine models are driven by increased proliferation of stem and progenitor cells in the BM, effective treatment requires normalization of this compartment. FACS analysis of stem and progenitor populations in the BM revealed that ruxolitinib treatment alone slightly decreased the most immature populations, LSK and LT-HSCs, but did not affect ST-HSCs and MPPs. Likewise, IMG-7289 alone had no significant effect on these populations. The low-dose combination, however, significantly decreased the percentage of all 4 stem and progenitor populations assayed: LSK, LT-HSCs, ST-HSCs, and MPPs (Fig. 6D).

We investigated whether the decrease in stem and progenitor cells evident by FACS analysis was also manifested by a decrease in the number of hematopoietic colonies arising from the BM of IMG-7289-, ruxolitinib-, or doubly treated mice. BM cells from control and treated *MxJak2^{V617F}* mice were cultured in methylcellulose containing erythropoietin, IL3, IL6, and SCF and colony growth scored on day 14. As single agents, neither IMG-7289 nor ruxolitinib caused a significant decrease in colony-forming unit (CFU) granulocyte, erythrocyte, monocyte, megakaryocyte (GEMM), CFU-GM, or burst-forming unit erythrocyte growth (Fig. 6E). IMG-7289 alone showed a nonsignificant increase in CFU-GM, which is consistent with the previously published observation by Sprussel et al that LSD1i causes an increase in monocytic cells.[10] By contrast, the low-dose combination significantly reduced both the most primitive, multilineage CFU-GEMM cells, as well as erythroid BFU-E burst formation. Thus, IMG-7289 and ruxolitinib synergize to curtail stem and progenitor cell expansion in a murine MPN model.

Ruxolitinib was approved for MPN patients mainly due to its often compelling effect on spleen size. Therefore, as expected, splenomegaly was already significantly ameliorated in ruxolitinib-treated mice, albeit with spleens remaining 4 to 5 times the normal size, while IMG-7289 alone did not lead to a significant reduction (Fig. 6F). Spleen size was further reduced by another 60% in mice receiving the combination therapy (Fig. 6F).

Discussion

Aberrant activation of JAK-STAT signaling through *JAK2*, *MPL*, or *CALR* mutations is the main contributor to the MPN phenotype. Consequently, JAK1/2 inhibitors were developed with the hope of efficiently managing symptoms as well as eliminating the malignant clone. While the JAK1/2 inhibitor ruxolitinib reduces splenomegaly and inflammation, thereby significantly improving patient quality of life, full molecular remissions are exceedingly rare. On the contrary, a recent report detailing acquisitions of novel, prognostically unfavorable mutations during ruxolitinib treatment, is reason for concern.[8] Thus, Ruxolitinib treatment so far has shown limited impact on the *JAK2^{V617F}* mutant clone.[3–7] This can be due either to insufficient JAK inhibition or because malignant clones do not depend exclusively on constitutive JAK2 activation. Crucially, the natural history of MPNs is largely unaffected by clinical JAK1/2 inhibition.
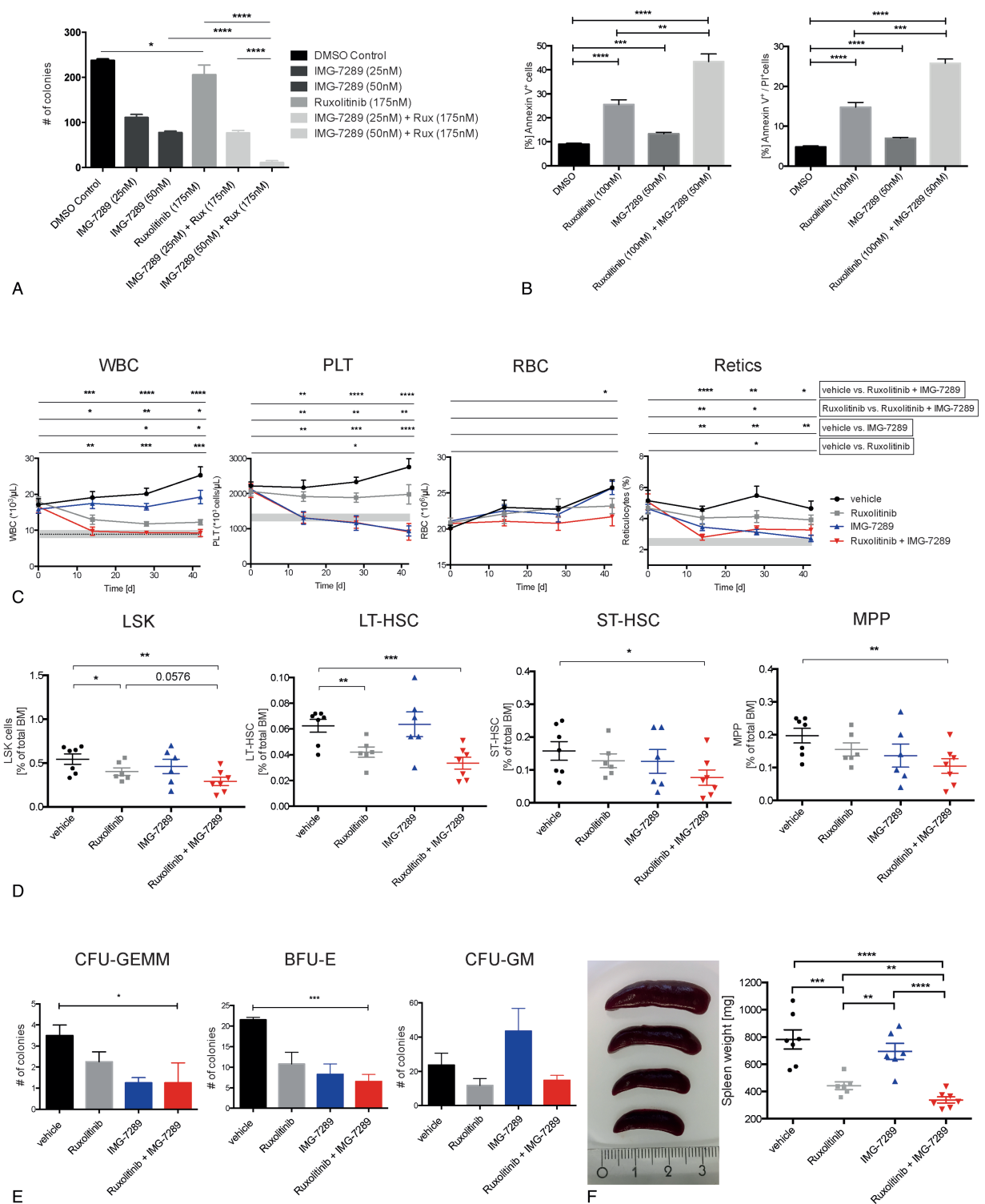
Figure 6. Jak1/2 inhibition synergizes in vitro and in vivo with LSD1 inhibition. (A) Number of colonies formed by SET-2 cells, treated either with DMSO, IMG-7289 (25 nM, 50 nM) or ruxolitinib (175 nM) alone or both drugs in combination, as indicated (n = 3 independent experiments). (B) Quantification of apoptosis in SET-2 cells, treated as indicated, detected with FACS for either Annexin V (left) or Annexin V and PI staining (right) (n = 2 independent experiments, each in duplicate). (C) Hematological parameters in peripheral blood of $Jak2^{V617F}$ mice treated either with vehicle, IMG-7289, ruxolitinib, or IMG-7289 and ruxolitinib (n = 6–9 mice per group). White blood cell (WBC, top left) count, platelet counts (PLT, top right), RBC count (bottom left), and reticulocytes (bottom right). Gray bars depict the normal range for each parameter (except for RBCs, where the normal range is below $10^7/\mu L$). (D) BM cells were stained with antibodies against a cocktail of lineage markers as well as against c-kit, Sca-1, CD34, Fc-γR, and Flt3/Flk2. Hematopoietic cell populations, defined as previously described,[51,52,55] are depicted as a percentage of total BM cells. Lineage$^-$, c-kit$^+$, Sca-1$^+$ (LSK) cells (left), long-term hematopoietic stem cell (LT-HSC, second to left), short-term hematopoietic stem cell (ST-HSC, second to right) and multipotent progenitor (MPP, right). n = 6 to 8, as indicated. (E) Colony formation of BM from treated $Jak2^{V617F}$ mice. Colony-forming unit (CFU) granulocyte, erythrocyte, monocyte, megakaryocyte (GEMM, left), burst-forming unit erythrocyte (BFU-E, middle), and CFU granulocyte, monocyte (CFU-GM, right). n = 2 to 3 (each in duplicate). (F) Spleen weight of treated $Jak2^{V617F}$ mice. n = 6 to 7, as indicated. (A–F) Mean and standard error of mean are shown. Statistical analysis was conducted using Student t tests with Welch correction. $^*P < 0.05$, $^{**}P < 0.01$, $^{***}P < 0.001$, and $^{****}P < 0.0001$. BM = bone marrow, RBC = red blood cell.

Here we use both a novel and 2 established mouse models of MPNs to explore the effects of inhibiting LSD1, a chromatin-modulating enzyme shown to be critical for normal myeloid maturation and for self-renewal of leukemia initiating cells. Each of these mouse models recapitulates essential features of MPNs including clonal expansion of mutant cells, increased inflammatory cytokines, and elevated peripheral cell counts including thrombocytosis, splenomegaly, and MF. In both $Jak2^{V617F}$ and in MPL^{W515L}-driven models, inhibition of LSD1 activity dramatically impacted the pathologic features of MPNs. Thrombocytosis and neutrophilia were reduced significantly (Fig. 1B and C), splenomegaly and splenic architecture (Fig. 2C and D) were improved, and inflammatory Cxcl5 levels lowered significantly (Fig. 2B, Fig. S1L, Supplemental Digital Content, http://links.lww.com/HS/A13). Similar effects have been reported in MPN mouse models treated with ruxolitinib although to varying degrees.[20] In addition, however, LSD1i significantly reduced MF and the mutant allele burden, effects not reported in these models with ruxolitinib.

Because LSD1 and JAK2 function in different intracellular pathways, we explored the possibility that their concurrent inhibition may yield synergistic effects. Indeed, low doses of IMG-7289 and ruxolitinib, which were suboptimally effective on their own, showed more than additive effects in combination (Fig. 6). As both the levels of side effects and the risk of selecting resistant clones may correlate with drug doses administered, the efficacy of a low-dose combination regimen in our preclinical setting warrants investigation of this therapeutic option.

The marked reduction in fibrosis by LSD1i the MPL^{W515L} MF model (Fig. 2F) is a novel and significant observation in this study. Fibrosis is among the most crucial determinants of disease course and morbidity in MF patients.[44] Interferon alpha is the only drug reported to reverse fibrosis in a subset of MPN patients when given early in the course of the disease.[45,46] The marked reduction of grade 3 fibrosis in the MPL^{W515L} mice suggests that LSD1i may reverse MF in patients in advanced stages of the disease.

The significant reduction in mutant allele frequency is another important in vivo effect of IMG-7289. We show that IMG-7289 induces apoptosis preferentially in mutant cells by several mechanisms including the enhanced activity of TP53, and, independently, due to the presence of a homozygous R248W mutation in the SET-2 cells used,[38] an increase in PUMA expression, and a concomitant reduction of BCL_{XL} levels. The pro-survival factor BCL_{XL}, which is overexpressed in PV patients,[32] may contribute to EPO-independent erythropoiesis, a pathognomonic feature of PV. BCL_{XL} overexpressing mutant cells may thus be exquisitely sensitive to reduction of BCL_{XL} levels by LSD1i. As PUMA induces apoptosis by binding BCL_{XL}, thereby dissociating the antiapoptotic BCL_{XL}-BAX complex,[47] selective sensitivity of MPN cells may be amplified by the concurrent repression of BCL_{XL} transcription and its functional inactivation by increased PUMA levels.

IMG-7289 also impairs the progression of mutant cells through the cell cycle. Cell cycle arrest following DNA damage is likewise TP53-mediated and may be more pronounced in the MPN clone due to $JAK2^{V617F}$-mediated accumulation of ROS and the subsequent induction of double-stranded DNA breaks.[48] Moreover, TP53 has been shown to be functionally inactivated in $JAK2^{V617F}$-positive cells by MDM2-mediated degradation.[49] Which of these mechanisms plays the greater role in reducing the fitness of mutant cells is not known but our observations admit the possibility that the mutant cell population might be

successfully eroded over time with the pharmacologic inhibition of LSD1 by IMG-7289.

In this study, we show that pharmacologic inhibition of LSD1 activity by the oral agent IMG-7289 in a preclinical MPN model affect several pathways that facilitate the selective growth advantage of the malignant clone (Fig. 7). IMG-7289 induces both cell cycle arrest and apoptosis of $JAK2^{V617F}$ mutant cells while concurrently reducing inflammation and fibrosis resulting in significantly prolonged survival of $Jak2^{V617F}$ mice.

Materials and methods

Generation Mx1cre-Jak2^{V617F} mice

The conditional floxed Jak2 ki mice, a generous gift by Jean-Luc Villeval, have been previously described.[15] Jak2-ki mice were crossed with *Mx1cre* transgenic mice (Tg(Mx1-cre)1Cgn: JAX stock No. 003556) to generate an inducible mutation. Double transgenic mice, which carry a WT $Jak2^{WT}$ and a mutated $Jak2^{V617F}$ allele ($Jak2^{V617F/WT}$), as well as the Mx1cre recombinase (called Mx-Jak2^{V617F}), were used for inhibitor treatment.

Jak2^{V617F} BM transplantation model

Murine BM was retrovirally transduced using an *MSCV-IRES-GFP-Jak2^{V617F}* vector and transplanted into lethally irradiated recipients as previously described.[21,22] Mice with established disease were treated with the LSD1 inhibitor IMG-7289 (45 mg/kg, q.d., oral gavage) for 14 days. Peripheral blood GFP levels were determined at the beginning and at the end of treatment.

IMG-7289 and ruxolitinib treatment and analysis of Mx1cre-Jak2^{V617F} mice

IMG-7289 or ruxolitinib in aqueous solution contained 0.5% Tween-80 and 0.5% carboxymethylcellulose (CMC). IMG-7289 and vehicle treatment groups were equal in age, sex, hematocrit, and leukocyte count at day 0 of treatment. IMG-7289 (45 mg/kg body weight) or vehicle (0.5% of both CMC and Tween-80) was administered daily by oral gavage for either 14, 42, or 56 consecutive days. Ruxolitinib (30 mg/kg body weight) was administered twice daily by oral gavage. Blood was drawn by retro-bulbar puncture and complete blood cell measurement performed (ADVIA 120, Siemens, Erlangen, Germany). BM was harvested by flushing both tibiae and 1 femur. One femur was used for histopathological analysis. Spleens were weighed then used for histopathology and for generating single cell suspensions.

MPL^{W515L} BM transplantation model

MPL^{W515L} BM transplantation experiments were performed as described previously.[50] Shortly, prestimulated c-kit enriched BM cells were subjected to 2 rounds of cosedimentation with viral supernatant containing *MSCV-hMPL^{W515L}-IRES-GFP* or empty *MSCV-IRES-GFP* control vector. A total of 1×10^6 cells (~25% to 40% GFP-positive, MPL^{W515L}-expressing cells) were injected into the tail veins of lethally irradiated syngeneic mice. At first signs of disease, mice were randomized based on WBC counts and GFP levels to begin treatment with the LSD1 inhibitor IMG-98 (5 mg/kg, q.d., oral gavage) or vehicle for 28 days. Mice were monitored daily for signs of illness and nonlethal bleeds were performed bi-weekly to follow-up disease progression.
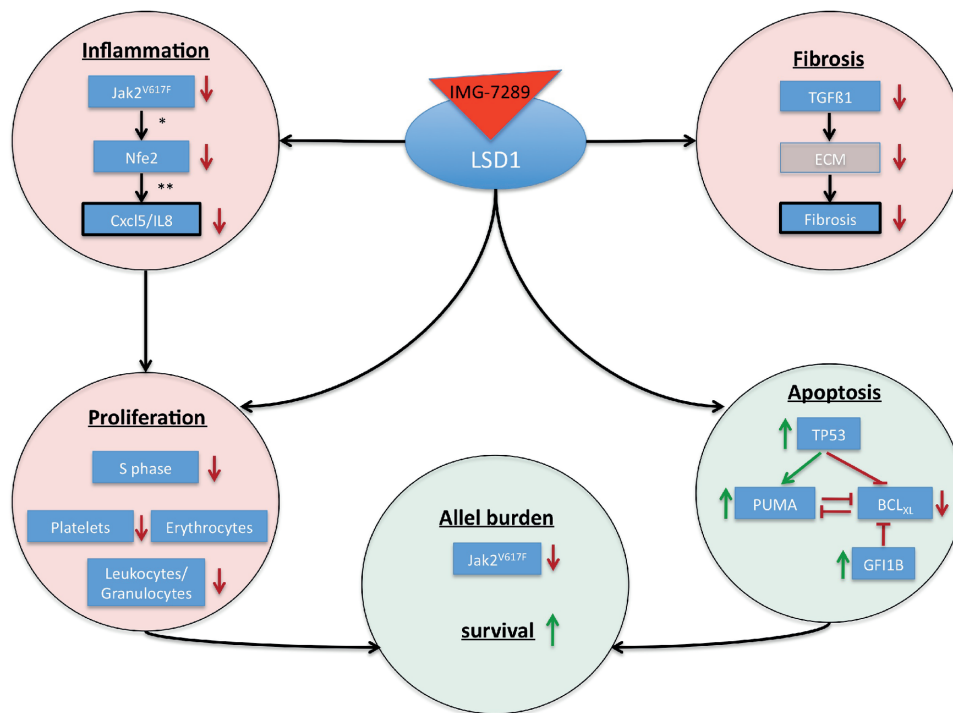
Figure 7. Mode of action of LSD1 inhibition in MPN. Model displaying the mode of action by which LSD1 inhibition affects inflammation, fibrosis, proliferation, apoptosis, and overall survival. ECM = extra cellular matrix. * = Skoda, unpublished, ** = Wehrle, Haematologica, 2013. MPN = myeloproliferative neoplasm.

Animal housing and protection

$Mx1cre\text{-}Jak2^{V617F}$ and $MSCV\text{-}IRES\text{-}GFP\text{-}Jak2^{V617F}$ mice were kept under specific pathogen-free conditions at the research mouse facility of the University Medical Center Freiburg. Experiments were performed in accordance with committee-approved animal protocols (Environment and Consumer Protection of the state Baden-Württemberg, Germany [G-13/100, G-17/43]).

MPL^{W515L} animal experiments were performed in accordance with Memorial Sloan Kettering Cancer Center Institutional Animal Care and Use Committee-approved animal protocol.

Histopathological analysis

Femur and spleen samples were fixed in 4% formalin ($Mx1cre\text{-}Jak2^{V617F}$ mice) or 4% paraformaldehyde (MPL^{W515L} mice) overnight. Femora were consecutively decalcified in 10% buffered ethylene-diamine tetra-acetic acid (EDTA), pH 7.2. Organs were embedded in paraffin as previously described.[26] Sections were either stained automatically with hematoxylin and eosin (H&E) or manually for reticulin fibers using silver impregnation method kit (Bio-Optica, Milano, Italy).

Cell line and in vitro treatment

The human cell lines SET-2 (ATCC 608) and HEK293 were cultured in RPMI or DMEM, respectively, supplemented with either 20% (SET-2) or 10% (HEK293) fetal bovine serum (FBS), 100 U/mL penicillin, and 0.1 mg/mL streptomycin. Cells were kept at a density of 5×10^5 to 10^6 cells/mL. The murine cell line Baf/3 was cultured in RPMI (10% FBS, 100 U/mL penicillin and 0.1 mg/mL streptomycin). Baf/3 WT and Baf/3 $Jak2^{V617F}$ cells were cocultured at a ratio of 1:1. IMG-7289 was dissolved in

DMSO and applied daily to cultured cells for up to 96 hours, as indicated. DMSO was applied to control cells at equal volumes.

Western blotting and antibodies

Murine BM cells were lysed in $5\times$ SDS buffer (250 mM Tris, pH 6.8, 10% SDS, 0.5% bromophenol blue, 50% glycerol, and 50 mM dithio-D-threitol) and subsequently sheared using a 26G needle. SET-2 cells were resuspended in lysis buffer (20 mM Tris—HCl, pH 7.5, 150 mM NaCl, 5 mM EDTA, pH 8.0, 1% Triton X-100) and homogenized for 10 min at 4°C by vigorous vortexing. Cell debris was removed by centrifugation. Protein concentrations were estimated by Bradford assay (Bio-Rad, Hercules, CA, USA, No. 500-0007) and lysates subjected to western blotting. The following primary antibodies were used: BCL_{XL} (CST, No. 2764), TP53 (CST, No. 9282), TP53-di-methyl-Lys370 (SAB, No. HW106), PUMA (D30C10) (CST, No. 12450), H3K4me3 (active motif, No. 39159), and H3K9me2 (active motif, No. 39239). Blots were stripped and re-probed for ß-Actin (Sigma-Aldrich, St. Louis, MO, USA, No. A5441) or total histone H3 (CST, Danvers, MA, USA, No. 9715) to control for equal loading. Immunocomplexes were detected by enhanced chemiluminescence and analyzed densitometrically using the ImageJ software.

FACS analysis of hematopoietic stem and progenitor cells

BM was stained with a cocktail against lineage markers (CD3, CD11b, B220, Ter119, and Ly6G/6C; BioLegend, San Diego, CA, USA), and for c-Kit (clone 2B8; eBioscience, Waltham, MA, USA), Sca-1 (clone D7; BioLegend), CD34 (clone MEC14.7; BioLegend), Fc-γ-II/III-R (clone 93; eBioscience), Thy1.1 (clone OX7; BioLegend), and Flt3 (clone A2F10; eBioscience). Stem and progenitor

cell subpopulations were identified as previously described[51–53]; gating strategies were determined by fluorescence minus one staining.[26]

Apoptosis and cell cycle analysis

Apoptosis was assessed with the "FITC Annexin V Apoptosis Detection Kit with PI" (BioLegend, No. 640914). Hoechst 33342 stating was used for cell cycle analysis.[27]

Colony assays

BM cells were seeded in methylcellulose media with EPO, IL3, IL6, and SCF (STEMCELL Technologies, Vancouver, Canada, MethoCult M3434) for CFU-GEMM, CFU-GM, and BFU-E assays and incubated for 12 days at 37°C, 5% CO_2. For correct identification of BFU-E, colonies were stained with benzidine.

Quantitative PCR/quantitative RT-PCR

$Jak2^{V617F}$ allele burden.
For each sample, 200 ng of murine PB leukocyte or BM gDNA was used and assayed in duplicate. The PCR strategy employed constitutes an adaptation of the assay optimized for $Jak2^{V617F}$ quantification on human DNA.[54] The reverse primers span the intron/exon boundary at the 3′ end of exon 13. One reverse primer (Jak2 all) quantitates both the wt and the V617F mutant allele while the other primer ($Jak2^{V617F}$) carries the single basepair mismatch and thus detects the V617F allele.

Common forward primer: 5′-CAGCAAGCATGATGAGTCA-GCTTT-3′
$Jak2^{V617F}$ reverse primer: 3′-AAGTCACCTCTCCTCTCATTC-ATTT-5′
$Jak2$ all reverse primer: 3′-CACCTCTCCTCTCATTCATTT-CGGT-5′

The ratio of mutated $Jak2^{V617F}$ to total $Jak2$ was determined and represented as percent mutated cells. As all cells are in a heterozygous state, the $Jak2$ mutant allele burden reaches a maximum of 50%. To indicate the percentage of cells carrying the mutant allele, maximal mutant allele burden was set at 100% indicating all cells carried the mutation.

Nfe2 expression. Reverse transcription of 200 ng of total BM RNA was performed using the TaqMan Reverse Transcription kit (Applied Biosystems, Foster City, CA, USA, No. 4368813). Murine Nfe2 mRNA expression was quantitated using the following reagents:

Forward primer, 5′-CTTTCTGGTGCTTGTCTCACTGAC-3′
Reverse primer, 5′-GGTGGCGTGAGTATACTTGAATTTG-3′

and probe, 6-FAM-ATCCAGAAAACCCC-MGBNFQ; murine ß-2-microglobulin was assays with an Assay on Demand (Applied Biosystems). Quantitative PCR assays were performed in duplicate using a LightCycler 480 (Roche, Basel, Switzerland). Differences in Nfe2 expression were determined using the $-\Delta\Delta CT$ method.

Cxcl5 determination

The Cxcl5 concentration in plasma of $Mx\text{-}Jak2^{V617F}$ mice was determined by ELISA (Thermo Scientific, Waltham, MA, USA, No. EMCXCL5), in plasma of MPL^{W151L} mice by Luminex Multiplex-Assay (Millipore, Burlington, MA, USA, MCYT-MAG-70K-PX32).

Statistical analysis

Data were analyzed with Student *t* tests. Survival analysis was conducted using Log-rank (Mantel-Cox) test. Densitometry was performed using the ImageJ software (National Institutes of Health, Bethesda, MD, USA).

References

1. Verstovsek S, Kantarjian H, Mesa RA, et al. Safety and efficacy of INCB018424, a JAK1 and JAK2 inhibitor, in myelofibrosis. *N Engl J Med* 2010; 363:1117–1127.
2. Pardanani A, Vannucchi AM, Passamonti F, et al. JAK inhibitor therapy for myelofibrosis: critical assessment of value and limitations. *Leukemia* 2011; 25:218–225.
3. Verstovsek S, Mesa RA, Gotlib J, et al. A double-blind, placebo-controlled trial of ruxolitinib for myelofibrosis. *N Engl J Med* 2012; 366:799–807.
4. Verstovsek S, Vannucchi AM, Griesshammer M, et al. Ruxolitinib versus best available therapy in patients with polycythemia vera: 80-week follow-up from the RESPONSE trial. *Haematologica* 2016; 101:821–829.
5. Vannucchi AM, Verstovsek S, Guglielmelli P, et al. Ruxolitinib reduces JAK2 p.V617F allele burden in patients with polycythemia vera enrolled in the RESPONSE study. *Ann Hematol* 2017; 96:1113–1120.
6. Deininger M, Radich J, Burn TC, et al. The effect of long-term ruxolitinib treatment on JAK2p.V617F allele burden in patients with myelofibrosis. *Blood* 2015; 126:1551–1554.
7. Harrison CN, Vannucchi AM, Kiladjian JJ, et al. Long-term findings from COMFORT-II, a phase 3 study of ruxolitinib vs best available therapy for myelofibrosis. *Leukemia* 2016; 30:1701–1707.
8. Newberry KJ, Patel K, Masarova L, et al. Clonal evolution and outcomes in myelofibrosis after ruxolitinib discontinuation. *Blood* 2017; 130: 1125–1131.
9. Yonal-Hindilerden I, Daglar-Aday A, Akadam-Teker B, et al. Prognostic significance of ASXL1, JAK2V617F mutations and JAK2V617F allele burden in Philadelphia-negative myeloproliferative neoplasms. *J Blood Med* 2015; 6:157–175.
10. Sprussel A, Schulte JH, Weber S, et al. Lysine-specific demethylase 1 restricts hematopoietic progenitor proliferation and is essential for terminal differentiation. *Leukemia* 2012; 26:2039–2051.

11. Kerenyi MA, Shao Z, Hsu YJ, et al. Histone demethylase LSD1 represses hematopoietic stem and progenitor cell signatures during blood cell maturation. *Elife* 2013; 2:e00633.

12. Niebel D, Kirfel J, Janzen V, et al. Lysine-specific demethylase 1 (LSD1) in hematopoietic and lymphoid neoplasms. *Blood* 2014; 124:151–152.

13. Harris WJ, Huang X, Lynch JT, et al. The histone demethylase KDM1A sustains the oncogenic potential of MLL-AF9 leukemia stem cells. *Cancer Cell* 2012; 21:473–487.

14. Schenk T, Chen WC, Gollner S, et al. Inhibition of the LSD1 (KDM1A) demethylase reactivates the all-trans-retinoic acid differentiation pathway in acute myeloid leukemia. *Nat Med* 2012; 18:605–611.

15. Hasan S, Lacout C, Marty C, et al. JAK2V617F expression in mice amplifies early hematopoietic cells and gives them a competitive advantage that is hampered by IFNalpha. *Blood* 2013; 122:1464–1477.

16. Kuhn R, Schwenk F, Aguet M, et al. Inducible gene targeting in mice. *Science* 1995; 269:1427–1429.

17. Hasselbalch HC. Perspectives on chronic inflammation in essential thrombocythemia, polycythemia vera, and myelofibrosis: is chronic inflammation a trigger and driver of clonal evolution and development of accelerated atherosclerosis and second cancer? *Blood* 2012; 119:3219–3225.

18. Jutzi JS, Pahl HL. The hen or the egg: inflammatory aspects of murine MPN models. *Mediators Inflamm* 2015; 2015:101987.

19. Pardanani A. JAK2 inhibitor therapy in myeloproliferative disorders: rationale, preclinical studies and ongoing clinical trials. *Leukemia* 2008; 22:23–30.

20. Pikman Y, Lee BH, Mercher T, et al. MPLW515L is a novel somatic activating mutation in myelofibrosis with myeloid metaplasia. *PLoS Med* 2006; 3:e270.

21. Wernig G, Mercher T, Okabe R, et al. Expression of Jak2V617F causes a polycythemia vera-like disease with associated myelofibrosis in a murine bone marrow transplant model. *Blood* 2006; 107:4274–4281.

22. Lacout C, Pisani DF, Tulliez M, et al. JAK2V617F expression in murine hematopoietic cells leads to MPD mimicking human PV with secondary myelofibrosis. *Blood* 2006; 108:1652–1660.

23. Tefferi A, Vaidya R, Caramazza D, et al. Circulating interleukin (IL)-8, IL-2R, IL-12, and IL-15 levels are independently prognostic in primary myelofibrosis: a comprehensive cytokine profiling study. *J Clin Oncol* 2011; 29:1356–1363.

24. Foudi A, Kramer DJ, Qin J, et al. Distinct, strict requirements for Gfi-1b in adult bone marrow red cell and platelet generation. *J Exp Med* 2014; 211:909–927.

25. Shivdasani RA, Rosenblatt MF, Zucker-Franklin D, et al. Transcription factor NF-E2 is required for platelet formation independent of the actions of thrombopoietin/MGDF in megakaryocyte development. *Cell* 1995; 81:695–704.

26. Kaufmann KB, Grunder A, Hadlich T, et al. A novel murine model of myeloproliferative disorders generated by overexpression of the transcription factor NF-E2. *J Exp Med* 2012; 209:35–50.

27. Jutzi JS, Bogeska R, Nikoloski G, et al. MPN patients harbor recurrent truncating mutations in transcription factor NF-E2. *J Exp Med* 2013; 210:1003–1019.

28. Wehrle J, Seeger T, Schwemmers S, et al. Transcription factor NF-E2 mediates expression of the cytokine IL8, a known independent predictor of inferioroutcome in MPN patients. *Haematologica* 2013; 98:1073–1080.

29. Goerttler PS, Kreutz C, Donauer J, et al. Gene expression profiling in polycythaemia vera: overexpression of transcription factor NF-E2. *Br J Haematol* 2005; 129:138–150.

30. Wang W, Schwemmers S, Hexner EO, et al. AML1 is overexpressed in patients with myeloproliferative neoplasms and mediates JAK2V617F-independent overexpression of NF-E2. *Blood* 2010; 116:254–266.

31. Uozumi K, Otsuka M, Ohno N, et al. Establishment and characterization of a new human megakaryoblastic cell line (SET-2) that spontaneously matures to megakaryocytes and produces platelet-like particles. *Leukemia* 2000; 14:142–152.

32. Silva M, Richard C, Benito A, et al. Expression of Bcl-x in erythroid precursors from patients with polycythemia vera. *N Engl J Med* 1998; 338:564–571.

33. Hosseini A, Minucci S. A comprehensive review of lysine-specific demethylase 1 and its roles in cancer. *Epigenomics* 2017; 9:1123–1142.

34. Huang J, Sengupta R, Espejo AB, et al. p53 is regulated by the lysine demethylase LSD1. *Nature* 2007; 449:105–108.

35. Han J, Flemington C, Houghton AB, et al. Expression of bbc3, a pro-apoptotic BH3-only gene, is regulated by diverse cell death and survival signals. *Proc Natl Acad Sci USA* 2001; 98:11318–11323.

36. Nakano K, Vousden KH. PUMA, a novel proapoptotic gene, is induced by p53. *Mol Cell* 2001; 7:683–694.

37. Bartke T, Siegmund D, Peters N, et al. p53 upregulates cFLIP, inhibits transcription of NF-kappaB-regulated genes and induces caspase-8-independent cell death in DLD-1 cells. *Oncogene* 2001; 20:571–580.

38. Zhao W, Du Y, Ho WT, et al. JAK2V617F and p53 mutations coexist in erythroleukemia and megakaryoblastic leukemic cell lines. *Exp Hematol Oncol* 2012; 1:15.

39. Zhang Y, Coillie SV, Fang JY, et al. Gain of function of mutant p53: R282W on the peak? *Oncogenesis* 2016; 5:e196.

40. Wang P, Qiu W, Dudgeon C, et al. PUMA is directly activated by NF-kappaB and contributes to TNF-alpha-induced apoptosis. *Cell Death Differ* 2009; 16:1192–1202.

41. Dumon S, Santos SC, Debierre-Grockiego F, et al. IL-3 dependent regulation of Bcl-xL gene expression by STAT5 in a bone marrow derived cell line. *Oncogene* 1999; 18:4191–4199.

42. Shi Y, Lan F, Matson C, et al. Histone demethylation mediated by the nuclear amine oxidase homolog LSD1. *Cell* 2004; 119:941–953.

43. Metzger E, Wissmann M, Yin N, et al. LSD1 demethylates repressive histone marks to promote androgen-receptor-dependent transcription. *Nature* 2005; 437:436–439.

44. Thiele J, Kvasnicka HM. Grade of bone marrow fibrosis is associated with relevant hematological findings—a clinicopathological study on 865 patients with chronic idiopathic myelofibrosis. *Ann Hematol* 2006; 85:226–232.

45. O'Neill C, Siddiqi I, Brynes RK, et al. Pegylated interferon for the treatment of early myelofibrosis: correlation of serial laboratory studies with response to therapy. *Ann Hematol* 2016; 95:733–738.

46. Pizzi M, Silver RT, Barel A, et al. Recombinant interferon-alpha in myelofibrosis reduces bone marrow fibrosis, improves its morphology and is associated with clinical response. *Mod Pathol* 2015; 28:1315–1323.

47. Ming L, Wang P, Bank A, et al. PUMA Dissociates Bax and Bcl-X(L) to induce apoptosis in colon cancer cells. *J Biol Chem* 2006; 281:16034–16042.

48. Marty C, Lacout C, Droin N, et al. A role for reactive oxygen species in JAK2 V617F myeloproliferative neoplasm progression. *Leukemia* 2013; 27:2187–2195.

49. Nakatake M, Monte-Mor B, Debili N, et al. JAK2(V617F) negatively regulates p53 stabilization by enhancing MDM2 via La expression in myeloproliferative neoplasms. *Oncogene* 2012; 31:1323–1333.

50. Kleppe M, Kwak M, Koppikar P, et al. JAK-STAT pathway activation in malignant and nonmalignant cells contributes to MPN pathogenesis and therapeutic response. *Cancer Discov* 2015; 5:316–331.

51. Akashi K, Traver D, Miyamoto T, et al. A clonogenic common myeloid progenitor that gives rise to all myeloid lineages. *Nature* 2000; 404:193–197.

52. Christensen JL, Weissman IL. Flk-2 is a marker in hematopoietic stem cell differentiation: a simple method to isolate long-term stem cells. *Proc Natl Acad Sci USA* 2001; 98:14541–14546.

53. Passegue E, Jamieson CH, Ailles LE, et al. Normal and leukemic hematopoiesis: are leukemias a stem cell disorder or a reacquisition of stem cell characteristics? *Proc Natl Acad Sci USA* 2003; 100 (suppl 1):11842–11849.

54. Jovanovic JV, Ivey A, Vannucchi AM, et al. Establishing optimal quantitative-polymerase chain reaction assays for routine diagnosis and tracking of minimal residual disease in JAK2-V617F-associated myeloproliferative neoplasms: a joint European LeukemiaNet/MPN&MPNr-EuroNet (COST action BM0902) study. *Leukemia* 2013; 27:2032–2039.

55. Passegue E, Wagers AJ, Giuriato S, et al. Global analysis of proliferation and cell cycle gene expression in the regulation of hematopoietic stem and progenitor cell fates. *J Exp Med* 2005; 202:1599–1611.